D11.2

An FFT Based Technique for Suppressing Narrow-Band Interference in PN Spread Spectrum Communications Systems[1]

Robert C. DiPietro

The MITRE Corporation, Bedford, MA 01730

Abstract

Analyses and performance predictions of an FFT based narrow-band interference suppression filter for use in spread spectrum communications systems are presented. The received baseband signal is processed in fixed-length blocks, transformed to the frequency domain with an FFT, filtered there by using an appropriate weighting, and then transformed back to the time domain. A general expression for the symbol matched filter signal-to-noise ratio (SNR) is given in terms of signal parameters and filter weighting coefficients. An optimal (maximum SNR) filtering scheme, as well as several suboptimal thresholding algorithms are discussed. Performance predictions, based on a realistic high frequency (HF) band interference model, are presented for these algorithms and FFT based architecture.

1.0 Introduction

Pseudonoise (PN) modulation in a digital communications system reduces the impact of interference caused by competing signals in the channel. The improvement is most evident when the offending signals are narrow-band relative to the PN modulated signal bandwidth. In this case the demodulation process, achieved by correlating the received signal with a locally generated version of the PN code sequence, spreads the narrow-band interference signal energy over the full PN bandwidth, while simultaneously collapsing the information bearing component to its original bandwidth. The narrow-band interference rejection afforded by PN modulation can be further enhanced by filtering the received wideband signal prior to demodulation [1]. Here the objective is to reduce the level of interference while minimizing the distortion on the desired signal. The filtering can be done in the time or frequency domain. A number of papers have explored adaptive filter designs in the time domain using linear prediction filters [2][3]. This paper looks at a frequency domain architecture, shown in figure 1, in which the noisy signal is processed in blocks of length N, transformed to the frequency domain with a complex FFT, filtered there to remove the interference by an appropriate weighting of the frequency domain values, and then transformed back to the time domain using an inverse FFT prior to demodulation. A similar architecture using SAW based DFT's was first considered by Das and Milstein [4].

[1]This work was funded by the Air Force Electronic Systems Division, AFSC, under contract no. F19628-86-C-0001. The project office was at the Rome Air Development Center, RADC/DCCD.

2.0 Signal Modeling and Symbol Correlation Signal-to-Noise Analysis

The input data stream, x_k, shown in figure 1 is the received baseband signal sampled at the chipping rate. These complex samples (I and Q or complex envelope representation) have three additive components, namely the PN signal sample, s_k, the broadband noise sample η_k, and the composite narrow-band interference sample, θ_k. Each component is assumed to be uncorrelated with the other two and to have a zero mean value. The individual component correlations are given by:

$$E[s_k s_m^*] = \begin{cases} 0 & k \neq m \\ S & k = m \end{cases} \qquad E[\eta_k \eta_m^*] = \begin{cases} 0 & k \neq m \\ \sigma^2 & k = m \end{cases}$$

$$E[\theta_k \theta_m^*] = r_{m-k},\ r_o = J \tag{1}$$

Here E [ ] is the expectation operator and * denotes complex conjugate.

Hence, the PN and noise samples are each temporally uncorrelated, and the narrow-band interferers are correlated. This model assumes binary phase shift keyed (BPSK) PN modulation of each data bit with a chip sequence of length M, and a different random chip sequence for each encoded symbol, each sequence uncorrelated with the others.

The input sample stream is grouped into blocks of length N (the FFT length) for suppression processing. The processing operation itself, namely the forward FFT, weighting of each frequency domain component by arbitrary weight α_k, and then transforming back to the time domain may be viewed as a linear transformation of the N point input block represented as a vector X, defined as the sum of the signal, noise, and interference component vectors. The i,k element of the N by N transformation matrix P follows from the DFT definition and figure 1.

$$P_{ik} = \frac{1}{N} \sum_{l=0}^{N-1} \alpha_l e^{j\frac{2\pi}{N}(i-k)l} \tag{2}$$

The N point filtered output vector $\hat{X}$ is then:

$$\hat{X} = PWX \tag{3}$$

Here W, a real diagonal matrix, W=diag $(w_0, w_1, \ldots, w_{N-1})$, has been added to allow for optional tapered time domain weighting to reduce frequency domain sidelobes.

CH2673-2/89/0000-1360 $1.00 © 1989 IEEE

The filtered vector is then returned to a serial data stream and sent through a symbol matched filter to remove the PN modulation. For analysis purposes, the matched filtering operation may be viewed as a correlation process applied to each block.[2] Letting V be a vector of length N composed of the received signal samples, s_k, scaled to unit magnitude, i.e., $V_k = s_k/|s_k|$, the correlation peak value is given by the inner product:

$$Z_{peak} = V^H \hat{X} = V^H P W X \tag{4}$$

The signal–to–noise–ratio (SNR) at the output of the correlator is given by [5]:

$$SNR = \frac{[E\{Z_{peak}\}]^2}{Var[Z_{peak}]} \tag{5}$$

Here Var[ ] is the variance operator and H denotes conjugate transpose

Straightforward (but tedious) calculation of the first and second moments of the correlator output based on the assumed statistical properties of the signal components and the characteristics of the transformation matrix P then yields the signal-to-noise ratio in the form:

$$SNR = \frac{(\frac{\Sigma_{k=1}^N w_k}{N})^2 |\Sigma_{k=1}^N \alpha_k|^2 S}{d_1 + d_2 + d_3}. \tag{6}$$

where

$$d_1 = \frac{\Sigma_{k=1}^N w_k^2}{N} \left\{ S \left[\Sigma_{k=1}^N \alpha_k^2 - \frac{|\Sigma_{k=1}^N \alpha_k|^2}{N} \right] \right\},$$

$$d_2 = \frac{\Sigma_{k=1}^N w_k^2}{N} \left\{ \sigma^2 \Sigma_{k=1}^N \alpha_k^2 \right\}, \text{ and}$$

$$d_3 = \frac{1}{N} \Sigma_{k=1}^N |\Theta_k \alpha_k|^2.$$

Here everything has been defined previously except Θ_k which is the kth FFT bin component of the narrow-band interference signal.

In this expression, the numerator shows the growth in signal power afforded by the spread spectrum processing gain. The first denominator term, d_1, is a "self noise" term that is analogous to that seen in linear prediction suppression processors [5] and is caused by chip skew. Note that this term vanishes for the case of no filtering (i.e., all α_k values unity). The second and third denominator terms, d_2 and d_3, are the residual broadband noise and narrow-band interference powers, respectively.

Leaving all α_k values at unity yields the pre-suppression SNR which, for the case of rectangular time domain weighting (i.e., all w_k values unity), is:

$$SNR = \frac{NS}{\sigma^2 + J} \tag{7}$$

Here Parseval's theorem has been used to define J, the average interference power.

[2]To simplify the analysis in this paper, the chipping sequence length M, is made equal to the FFT length N, and is aligned such that only one data symbol is present in each block. The approach here may be extended to cover the case of offset processing blocks and different lengths using matrix partitioning techniques.

$$\frac{1}{N^2} \Sigma_{k=1}^N |\Theta_k|^2 = \frac{1}{N} \Sigma_{k=1}^N |\theta_k|^2 = J \tag{8}$$

This is the expected intuitive result, showing an N-fold processing gain factor increase of the original input SNR value at the symbol correlator output. The ratio of this expression to a filtered scenario defines the improvement factor used to assess suppression performance.

3.0 Maximum SNR Algorithm

Having obtained a general SNR expression (eq. 6) valid for any fixed FFT length, N, and arbitrary frequency domain weight values, α_k, the obvious approach to finding weights that maximize this expression is to determine derivatives of this equation with respect to each of the N α_k values and set the resulting equations to zero. If this is done for the case of untapered time domain weighting, the ratio of the kth and lth frequency domain weight is given by:

$$\frac{\alpha_k}{\alpha_l} = \frac{S + \sigma^2 + \frac{|\Theta_l|^2}{N}}{S + \sigma^2 + \frac{|\Theta_k|^2}{N}} \tag{9}$$

The optimal weights are therefore defined in relation to each other. If the lth cell is chosen such that little or no narrow-band energy is present, the ratio becomes:

$$\frac{\alpha_k}{\alpha_l} = \frac{N(S + \sigma^2)}{N(S + \sigma^2) + |\Theta_k|^2} \tag{10}$$

As the PN and background noise signals are each uncorrelated, they will experience a factor N power growth in the forward FFT. Therefore the weight ratio is recognized as the quotient of the lth cell squared magnitude to the kth cell squared magnitude. Denoting the mth FFT cell by $Y(m)$, the optimal weight ratio becomes:

$$\frac{\alpha_k}{\alpha_l} = \frac{|Y(l)|^2}{|Y(k)|^2} \tag{11}$$

Finally noting from eq. 6 that any fixed scaling of the weights will yield the same SNR, α_l may be set to unity, hence the α_k weight yielding the maximum SNR value is determined as the ratio of the selected lth reference cell to the kth cell squared magnitude. Choosing a reference cell containing no interferers is simply a convenience that forces all the weights to be less than unity thereby avoiding large values that may cause dynamic range problems in the inverse FFT. However any cell may be selected as the reference cell yielding the same theoretical results.

This "maximum SNR" algorithm sets weights that are inversely proportional to the total power contained in that FFT cell. Hence cells containing very large interference values will nearly be eliminated. This suggests some simpler ad hoc algorithms discussed in the next section. Simulation results using this "maximum SNR" algorithm will be presented in section 4.

4.0 Thresholding Algorithms

The "maximum SNR" algorithm requires a complex multiply for each of the N frequency domain cells as well as a division to determine each weight. As discussed below, the distribution of interferer powers (from either the model or the real world data on which it is based) suggests that only a small number of frequency domain cells contain nearly

all the interference power within the band. From this observation, one possible suboptimal strategy would be to set the weights on all "large" cells to zero, while leaving the others at unity. This approach [4] is appealing in that the multiplier is replaced by a simple gating circuit. The obvious problem is to determine what constitutes a "large" interferer. One way is to establish a threshold level and declare any cell magnitude exceeding this level "large" hence removing it by gating. The level for this "threshold excision" algorithm may be set on the basis of knowledge of the interference distribution or some other rule of thumb, such as setting the level to excise a fixed percentage of the cells or total interference power.

The thresholding idea may be used in other ways. Any cell magnitude that exceeds the threshold may be clipped to the threshold level. Again this "threshold-clipping" technique may be implemented with no multipliers. Another variation would set any cell value exceeding the threshold to the background noise level, effectively whitening the interference spectrum. This "threshold whitening" approach will yield improved results (as shown by the example below) in that small magnitude interferers exceeding the threshold will only be reduced to the background level, hence retaining most of the signal energy. The one drawback with this approach is that an estimate of the background noise level must be made, complicating the algorithm.

5.0 Interference Characteristics

To quantify the improvements that this suppression technique can achieve, a recently developed model which predicts the amplitude distribution of narrow-band interference in the high frequency (HF) (i.e., 3-30 MHz) radio band is used [6]. The model is based on measured interference data taken in Europe [7] and may be extrapolated to different locations, seasons, and time-of-day with the proper choice of parameters. These include the maximum power of any in-band interferer, the noise figure of the environment, and the expected density of interferers. This last parameter means that if the selected frequency region, (the total bandwidth of the spread spectrum signal in our case), is broken down into a large number of narrow frequency bands, (as is achieved with the FFT in the processor), then the fraction of such bins containing narrow-band interference energy (in addition to background thermal noise), defines the interferer density. In Europe (the most severe environment) this density is nearly unity, while in the United States the value is in the range of 0.1-0.2. The key empirical observation upon which the model is based is that the logarithm of the probability of a particular interferer power level being exceeded in a given narrow frequency bin (i.e., 1.0 - power cumulative distribution function) varies linearly with the interference power expressed in dB. This implies that a very few resolution cells will contain the major portion of the total interference power. For the test example discussed in section 6, the model predicts a minimum and maximum interferer power of -111 dBm and -50 dBm respectively. If a 16,384 point FFT is used, then only a single cell will contain the large (-50 dBm) interferer. This corresponds to an exceedence probability of $1/16384 = 0.000061$. However, following this log-linearity relationship, the power level corresponding to an increased exceedence probability of 0.01 is -82.05 dBm. Hence, only 1 percent, or 164 out of the 16,384 cells can be expected to have powers above this level. The remaining 99 percent will contain interferer power values that are more than 32.05 dB down from the peak interference level of -50 dBm. At 10 percent exceedence, the power level is -96.5 dBm, hence 90 percent of the bins will have interferer powers more than 46.5 dB below the peak.

6.0 SNR Performance Predictions

In this section theoretical performance predictions are calculated from the generalized SNR relationship (eq. 6) using the various suppression algorithms in the context of a worst case interference environmental model based on European-Summer evening conditions. For these examples a 16,384 point FFT is used as well as a 16,384 chip symbol length. The total available processing gain is therefore 42 dB. The PN signal level is placed 26 dB below the background noise, hence the maximum available SNR available at the correlator output is -26 dB + 42 dB = 16 dB which is quite adequate for low error rate data demodulation of BPSK or DPSK encoded symbols. This maximum SNR would occur with no narrow-band interferers present and hence no filtering. The interference model assumes a total signal bandwidth of 1.024 MHz, an environmental noise figure of 45 dB, and a maximum interferer power level of -50 dBm. Each of the 16K frequency domain resolution cells (Δf=1.024 MHz/16384=62.5 Hz) is assumed to contain a narrow-band interferer, the smallest being equal to the noise floor (-111 dBm in the 62.5 Hz resolution bandwidth). The interferer power levels in each cell will then range between the noise floor and the maximum level of -50 dBm in accordance with the amplitude distribution predicted by the model. The total integrated interference power is -45.5 dBm. Having given every cell an interferer power level, each 62.5 Hz cell is then assigned a random position in the 1.024 MHz spectrum. A spectral plot of the resulting interference model is shown in figure 2.

The post suppression SNR values are plotted in figure 3 for the three thresholding alogrithms discussed in the previous section. Both actual SNR values and SNR improvement factors are shown in the two ordinate scales. Instead of being plotted with respect to absolute threshold level, the resulting fraction of cells exceeding a given threshold is chosen as an abscissa. For example, a 0.4 fraction implies that the threshold level is set so that 0.4 x 16384 = 6554 cells exceed the level. For reference purposes, the "maximum SNR algorithm" value (12.3 dB) is shown as well. These results show the performance of the threshold algorithms to be within a few dB of the interferer free value (16 dB) at the correct threshold level. The threshold whitening algorithm is the most robust but does of course require knowledge of the background level. The threshold clipping technique shows poorer performance at low exceedence values when compared to the excision and whitening algorithms. The excision technique works nearly as well as whitening at low exceedance levels. However, if too much of the band is excised, the performance will start to decline as the marginal additional reduction in very low level interferer values is offset by losses in signal power, hence, a reduction in SNR.

7.0 Conclusions

Analyses and performance predictions for an FFT based narrow-band interference suppression processor have been

given. Several algorithms have been considered and a realistic interference model has been used to assess performance.

References

1. M. J. Bouvier, Jr., The Rejection of Large CW Interferers in Spread-Spectrum Systems **COM-26** (February 1978), IEEE Trans. Communications.
2. R. A. Iltis and L. B. Milstein, Performance Analysis of Narrow-Band Interference Rejection Techniques in DS Spread-
   Spectrum Systems **COM-32** (November 1984).
3. E. Masry, Closed-Form Analytical Results for the Rejection of Narrow-Band Interference in PN Spread-Spectrum Systems– Part I: Linear Prediction Filters **COM-32** (August 1984), IEEE Trans. Communications.
4. L. B. Milstein and P. K. Das, An Analysis of a Real-Time Transform Domain Filtering Digital Communication System–
   Part I: Narrow-Band Interference Rejection **COM-28** (June 1980), IEEE Trans. Communications.
5. J. W. Ketchum and J. G. Proakis, Adaptive Algorithms for Estimating and Suppressing Narrow-Band Interference in PN Spread-Spectrum Systems **COM-30** (May 1982), IEEE Trans. Communications.
6. B. D. Perry and R. Rifkin, Interference and Wideband HF Communications (1987), Proc. Fifth Ionospheric Effects Symposium, Springfield, VA.
7. T. J. Moulsley, HF Data Transmission in the Presence of Interference (1985), IEE Conference Publication 245: Third International Congress on HF Communications Systems and Techniques, London, UK.

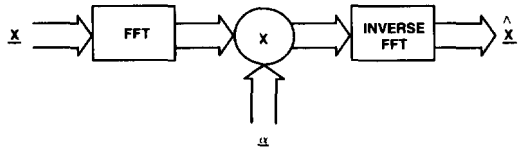

Figure 1. FFT BASED SUPPRESSION FILTER ARCHITECTURE

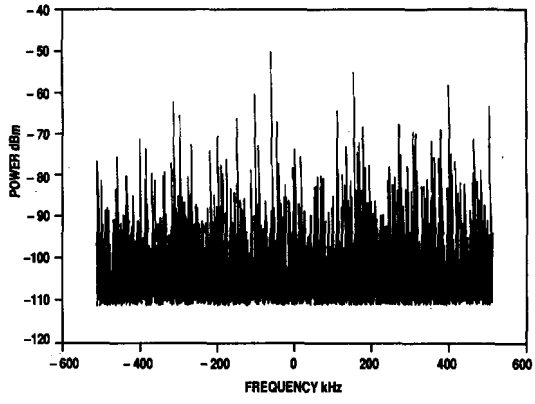

Figure 2. BASEBAND HF INTERFERENCE SPECTRUM (FROM MODEL)

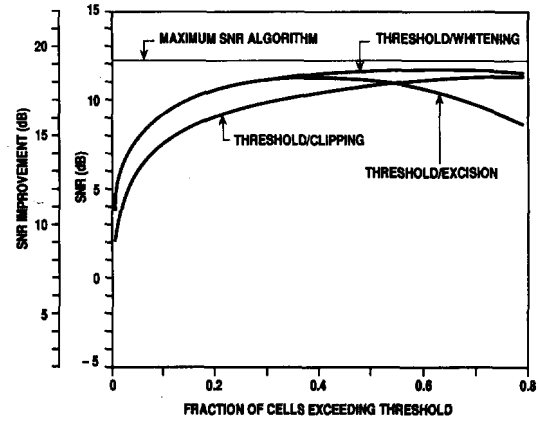

Figure 3. PERFORMANCE PREDICTIONS FOR EUROPE — SUMMER EVENING CONDITIONS